Title

Nicotinamide Adenine Dinucleotide Phosphate Oxidase Promotes Glioblastoma Radiation Resistance in a Phosphate and Tensin Homolog-Dependent Manner.

Journal

Antioxidants & Redox Signaling, 39(13-15)

Authors

Ludwig, Kirsten
Le Belle, Janel
Muthukrishnan, Sree
et al.

Publication Date

2023-11-01

DOI

10.1089/ars.2022.0086

Peer reviewed

ANTIOXIDANTS & REDOX SIGNALING
Volume 39, Numbers 13–15, 2023

DOI: 10.1089/ars.2022.0086

FORUM ORIGINAL RESEARCH COMMUNICATION

Nicotinamide Adenine Dinucleotide Phosphate Oxidase Promotes Glioblastoma Radiation Resistance in a Phosphate and Tensin Homolog-Dependent Manner

Kirsten Ludwig,[1,*] Janel E. Le Belle,[1,2] Sree Deepthi Muthukrishnan,[1] Jantzen Sperry,[1] Michael Condro,[1] Erina Vlashi,[3,4] Frank Pajonk,[3,4] and Harley I. Kornblum[1,4]

Abstract

Aims: The goal of this study was to determine whether nicotinamide adenine dinucleotide phosphate (NADPH) oxidase (NOX)-produced reactive oxygen species (ROS) enhance brain tumor growth of glioblastoma (GBM) under hypoxic conditions and during radiation treatment.
Results: Exogenous ROS promoted brain tumor growth in gliomasphere cultures that expressed functional phosphate and tensin homolog (PTEN), but not in tumors that were PTEN deficient. Hypoxia induced the production of endogenous cytoplasmic ROS and tumor cell growth *via* activation of NOX. NOX activation resulted in oxidation of PTEN and downstream protein kinase B (Akt) activation. Radiation also promoted ROS production *via* NOX, which, in turn, resulted in cellular protection that could be abrogated by knockdown of the key NOX component, p22. Knockdown of p22 also inhibited tumor growth and enhanced the efficacy of radiation in PTEN-expressing GBM cells.
Innovation: While other studies have implicated NOX function in GBM models, this study demonstrates NOX activation and function under physiological hypoxia and following radiation in GBM, two conditions that are seen in patients. NOX plays an important role in a PTEN-expressing GBM model system, but not in PTEN-nonfunctional systems, and provides a potential, patient-specific therapeutic opportunity.
Conclusion: This study provides a strong basis for pursuing NOX inhibition in PTEN-expressing GBM cells as a possible adjunct to radiation therapy. *Antioxid. Redox Signal*. 39, 890–903.

Keywords: NADPH oxidase, PTEN, glioblastoma, glioma, radiation, hypoxia, p22phox

Introduction

Glioblastoma (GBM) is a devastating disease, with a median survival of only 12–15 months. While the current standard of care of maximal surgical resection followed by radiation and chemotherapy with temozolomide prolongs life, tumors virtually always recur (Vilar et al., 2022). The mechanisms of this recurrence are multifaceted and may include cellular plasticity that is induced by chemotherapy and radiotherapy, as well as stem-like cells within tumors that are inherently resistant to these treatments, the so-called glioma stem cell (GSC) (Ludwig and Kornblum, 2017).

Although the cell of origin of GSC is unclear and potentially varied, these cells have some of the properties of neural stem cells (NSC), including their ability to self-renew and grow as gliomaspheres in a relatively simple, defined medium under the mitogenic control of added epidermal growth factor (EGF) and basic fibroblast growth factor (FGF) (Hemmati et al., 2003). Prior work in NSC biology has proven a role for the activation of the phosphoinositide 3-kinase (PI3K)/protein kinase B (Akt) pathway in normal NSC proliferation, including self-renewal, and maintenance of neurogenesis (Groszer et al., 2006; Groszer et al., 2001).

[1]The Intellectual and Developmental Disabilities Research Center and the Department of Psychiatry and Biobehavioral Sciences, Departments of [2]Neurosurgery and [3]Radiation Oncology, David Geffen School of Medicine at UCLA, Los Angeles, California, USA.
[4]Jonsson Comprehensive Cancer Center, University of California, Los Angeles, California, USA.
Current affiliation: Kaiser Permanente Bernard J. Tyson School of Medicine, Pasadena, California, USA.

An earlier draft of this article was posted as a preprint at bioRxiv (DOI: 10.1101/2022.06.16.496502).

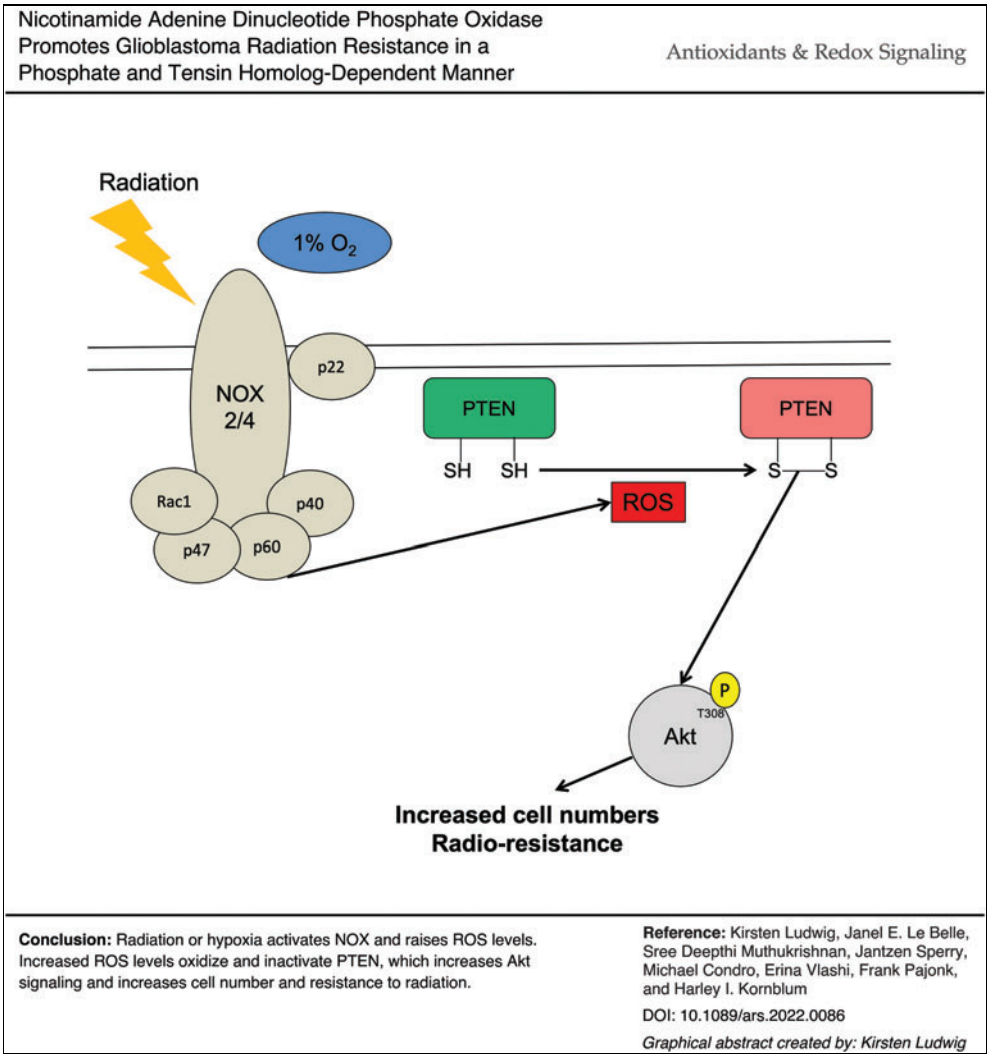

Color images are available online.

One means by which exogenous factors can influence this pathway is through the activation of the nicotinamide adenine dinucleotide phosphate (NADPH) oxidase (NOX) complex. NOX is found in abundance in many cell types, and its activation in neutrophils results in killing of the engulfed bacteria (Vermot et al., 2021). In NSC, as well as a variety of cancers, NOX is activated by growth factors and other means, to oxidatively inactivate the phosphate and tensin homolog (PTEN) protein, resulting in enhanced Akt and mammalian target of rapamycin (mTOR) activity (Le Belle et al., 2014; Le Belle et al., 2011).

Innovation

While other studies have implicated nicotinamide adenine dinucleotide phosphate (NADPH) oxidase (NOX) function in glioblastoma (GBM) models, the current study demonstrates NOX activation and function under physiological hypoxia and following radiation in GBM, two conditions that are clinically relevant. NOX plays an important role in a phosphate and tensin homolog (PTEN)-expressing GBM model system, but not in PTEN-nonfunctional systems, and provides a potential, patient-specific therapeutic opportunity.

The GBM microenvironment is primed to activate NOX, given the common occurrence of hypoxia and the presence of several growth factors and cytokines that are often associated with GBM (Rodriguez et al., 2022). Furthermore, radiation, a mainstay treatment modality for GBM, has been demonstrated to activate NOX (Mortezaee et al., 2019). Therefore, we hypothesized that NOX activation could play an important role in GBM growth and resistance to radiation therapy. Indeed, a prior report using model systems has provided some evidence for the former (Cao et al., 2022; Su et al., 2021). In this study, we examine the role of NOX activation in GBM cells and found that both hypoxia and radiation induce NOX activity to inactivate PTEN, enhance Akt phosphorylation, and promote survival (Graphical Summary Illustration). Reducing NOX activity resulted in slower tumor growth *in vivo* and enhanced radiosensitivity in PTEN-expressing GBM tumors. These findings suggest that inhibition of NOX activation is a potential therapeutic target in PTEN-functional GBM.

Results

Prior work has shown that modestly elevated reactive oxygen species (ROS) levels (between one and two-fold increase over endogenous levels) promote proliferation in

cancer and nontransformed cells, including neural progenitors (Le Belle et al., 2014; Le Belle et al., 2011). Using primary GBM lines, we found that cells with higher endogenous ROS levels significantly correlated with faster doubling time (Fig. 1A), suggesting that ROS may play a role in regulating cell numbers. Since this is a correlation and does not show causation, we decided to directly test our hypothesis. We have previously shown that ROS-induced proliferation in NSC occurs in a PI3K/Akt-dependent manner (Le Belle et al., 2011). In GBM, we found that treating cells that express functional PTEN with hydrogen peroxide (H_2O_2) (Supplementary Fig. S1A–C) resulted in increased cell numbers (Fig. 1B and Supplementary Fig. S2A–C).

In contrast, treatment of lines that lack functional PTEN with H_2O_2 resulted in no significant changes (Fig. 1B and Supplementary Fig. S2D–F), despite elevated ROS levels (Fig. 1C) in both PTEN-functional (Supplementary Fig. S3A–C) and PTEN-nonfunctional (Supplementary Fig. S3D–F) lines. Conversely, decreasing ROS levels *via* the antioxidant *N*-acetylcysteine (NAC) (Fig. 1C) resulted in decreased cell numbers in PTEN-functional lines with no change in PTEN-nonfunctional lines (Fig. 1B). Because PTEN function may not be the only difference between these lines, we used short hairpin RNA (shRNA) to knock down PTEN (Supplementary Fig. S4A, B). Treatment of cultures with the PTEN shRNAs that efficiently knocked down PTEN protein (sh1 and sh2) resulted in increased cell numbers, while the two constructs that failed to significantly knock down PTEN (sh3 and sh4) produced no functional effect (Supplementary Fig. S4A–C).

Furthermore, knocking down PTEN prevented the ROS-induced increase in cell numbers in all three PTEN-functional lines (Fig. 1D and Supplementary Fig. S5A–C), with little effect in the three PTEN-nonfunctional lines (Supplementary Fig. S5D–F). Similarly, lowering ROS levels *via* NAC decreased cell numbers only in control cells, but not in the PTEN knock down (KD) cells (Fig. 1D and Supplementary Fig. S5). No difference in ROS levels was found between the shCON and shPTEN groups (Fig. 1E and Supplementary Fig. S6A–F), suggesting that the changes are directly connected to PTEN. Taken together, these data support a role for ROS producing increased cell numbers in patient-derived GBM lines in a PTEN-dependent manner.

Increased ROS levels, such as addition of H_2O_2, have been shown to oxidize PTEN resulting in its reversible inactivation due to the creation of covalent disulfide bonds between cysteine residues (Lee et al., 2002). However, this oxidation event has rarely been documented in cells under biologically relevant conditions, such as hypoxia. Cancer cells are often found in hypoxic environments, which have been shown to paradoxically increase ROS levels (Rodriguez et al., 2022). To address the effects of hypoxia on ROS production, GBM cells were grown under low oxygen (1% O_2) or room air oxygen concentration as described in the Materials and Methods section and then subsequently examined. Incubation in low oxygen resulted in PTEN oxidation and increased Akt phosphorylation (Fig. 2A and Supplementary Fig. S7A, B) pointing to PTEN inactivation under hypoxic conditions.

Low oxygen conditions also resulted in increased ROS levels in both control and PTEN-knockdown cells, but the hypoxia-induced increase in cell numbers was only observed in the PTEN-functional lines with little effect on the PTEN-knockdown lines (Fig. 2B, C and Supplementary Figs. S8 and S9). Furthermore, when PTEN-functional and PTEN-nonfunctional lines were grown under hypoxic conditions, only the PTEN-functional lines increased in cell numbers, with no significant effect on PTEN-nonfunctional lines (Fig. 2D, E and Supplementary Fig. S10), although ROS levels universally increased under hypoxia (Supplementary Figs. S11A, B and S12A–F). Together these observations suggest that PTEN inactivation by the hypoxia-induced ROS might be driving the enhanced cell numbers of PTEN-functional cells under low oxygen conditions.

When PTEN-functional cells grown in low oxygen were treated with either NAC or the NOX inhibitor, apocynin (APO), it prevented the hypoxia-induced increase in cell numbers, again suggesting a role for ROS in this response and that NOX activation might contribute to the increased ROS levels. Treating cells with H_2O_2 under hypoxic conditions did not further increase cell numbers, suggesting that hypoxia results in a level of ROS that maximally increases cell numbers. Treatment with the PI3K inhibitor, LY294002 (LY), also prevented the hypoxia-induced increase in cell numbers, independent of ROS levels in PTEN-functional and PTEN-nonfunctional lines (Fig. 2D, E and Supplementary Figs. S11A, B and S12A–F).

When PTEN-functional cells were grown under low oxygen, PTEN was oxidized, and this was accompanied by an increase in Akt phosphorylation (Fig. 2F), which was prevented by NAC or APO treatment (Fig. 2F and Supplementary Fig. S13A, B). Importantly, LY treatment of hypoxic

FIG. 1. ROS-induced proliferation requires PTEN. (A) The Pearson correlation coefficient of endogenous ROS levels with relative doubling time in HK157, HK217, HK229, HK296, HK350, HK351, HK374, HK382, and HK393 cells. $p = 0.003$. **(B)** Changes in cell number were determined with a CCK-8 assay following treatment with 10 μM H_2O_2 or 1 mM NAC for 5 days in three PTEN-functional lines (HK157, HK339, and HK374) and three PTEN-nonfunctional lines (HK217, HK229, and HK296). Average values of all three lines were used to calculate data. $n = 3$, *dots* represent individual cell lines. $^{**}p < 0.1$, $^{****}p < 0.001$. **(C)** Changes in ROS levels were determined with CellROX Green following treatment with 10 μM H_2O_2 or 1 mM NAC for 5 days in three PTEN-functional lines (HK157, HK339, and HK374) and three PTEN-nonfunctional lines (HK217, HK229, and HK296). Average values of all three lines were used to calculate data. $n = 3$, *dots* represent individual cell lines. $^{****}p < 0.001$. **(D)** Changes in cell number were determined with a CCK-8 assay following shCON or shPTEN treatment with 10 μM H_2O_2 or 1 mM NAC for 5 days in three PTEN-functional lines (HK157, HK339, and HK374) and three PTEN-nonfunctional lines (HK217, HK229, and HK296). Average values of all three lines were used to calculate data. $n = 3$, *dots* represent individual cell lines. $^{**}p < 0.1$, $^{****}p < 0.001$. **(E)** Changes in ROS levels were determined with CellROX Green following shCON or shPTEN treatment with 10 μM H_2O_2 or 1 mM NAC for 5 days in three PTEN-functional lines (HK157, HK339, and HK374) and three PTEN-nonfunctional lines (HK217, HK229, and HK296). Average values of all three lines were used to calculate data. $n = 3$, *dots* represent individual cell lines. $^{****}p < 0.001$. CCK-8, Cell Counting Kit-8; H_2O_2, hydrogen peroxide; NAC, *N*-acetylcysteine. Color images are available online.

cells resulted in diminished Akt phosphorylation but did not prevent PTEN oxidation (Fig. 2F and Supplementary Fig. S13A, B). LY treatment also resulted in decreased cell numbers, although it had no effect of ROS levels (Fig. 2D, E and Supplementary Figs. S11A, B and S12A–F).

These findings suggest that the ROS-induced response may be dependent on the oxidation and inactivation of PTEN resulting in an increase in activation of the Akt pathway. Altogether, our data suggest that elevated ROS levels, whether *via* exogenous administration of H_2O_2 or induction of ROS under low oxygen conditions, oxidatively inactivate PTEN, resulting in enhanced Akt activity, and a subsequent increase in GBM cell numbers. The observation that APO, an inhibitor of NOX, which is a major contributor to intracellular ROS production (Mortezaee et al., 2019), recapitulates the effects of NAC led to the hypothesis that NOX activity may be involved.

NOX is a complex of proteins with several different isotypes to each component. NOX2 and p22 are localized to the

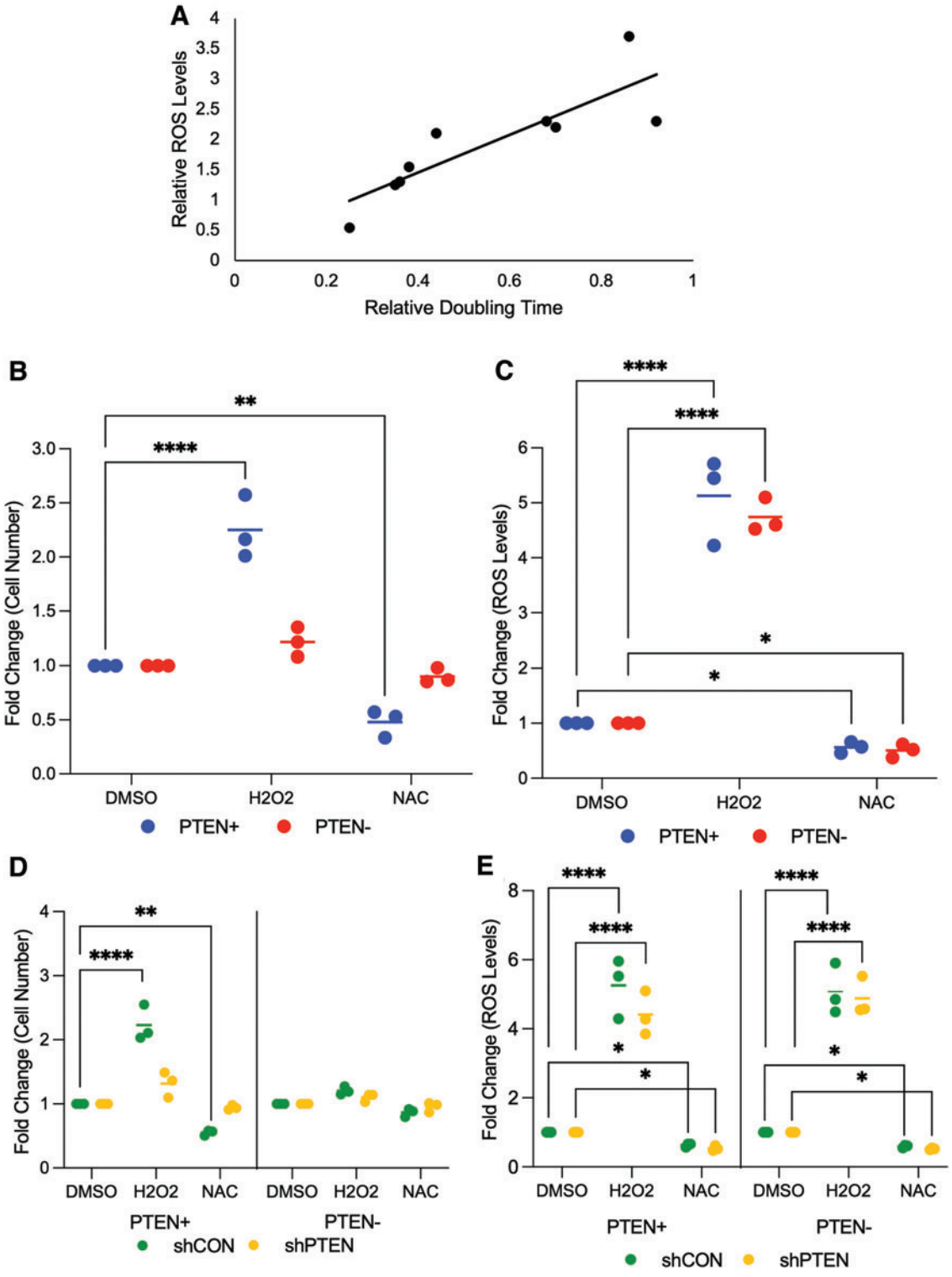

cellular membrane, and upon activation of Rac1, the cytosolic components of NOX (p40, p47, and p60) translocate to the membrane-bound complexes. This binding results in activation of NOX and generation of ROS. There are five different isotypes of NOX, as well as two isotypes of dual oxidase (DUOX), all of which produce superoxide, which is quickly converted to H_2O_2 (Mortezaee et al., 2019). In our lines, all components of the NOX complex were expressed regardless of the PTEN status, with NOX4 having the highest expression in both lines (Fig. 3A). NOX4 is unique among the family of proteins, as it does not require the cytosolic components to become activated, only membrane-bound p22 (Mortezaee et al., 2019).

Analysis of GlioVis data (Bowman et al., 2017) showed that CYBA (NOX2, P04839), CYBB (p22, P13498), and NOX4 (Q9NPH5) are all upregulated in GBM relative to non-tumor tissue (Fig. 3B). To directly address the role of NOX in our observations, we targeted p22 with shRNA (Supplementary Fig. S14A–C), given its role in the activation of both, NOX2 and NOX4. Knockdown of p22 in a PTEN-functional line resulted in decreased cell numbers (Fig. 3C and Supplementary Fig. S14D) and ROS levels (Supplementary Figs. S14E and S15A). Our data suggest that the effects of p22 knockdown are most likely due to its NOX activity, as the addition of APO had little effect on cell numbers, while H_2O_2 partially rescues the phenotype (Fig. 3C).

The lack of complete rescue is most likely due to the transient effect of H_2O_2 in a cell that has constitutively lower ROS levels due to the absence of p22. It is also possible that p22 plays a role in other functions beside ROS production. Knockdown of p22 in a PTEN-nonfunctional line did decrease ROS levels (Supplementary Fig. S15) but had minimal effect on cell numbers (Fig. 3C), highlighting the importance of PTEN in this pathway. Similar effects were observed with the three different shp22 constructs that resulted in 60% or more knockdown, while treatment with ineffective constructs had no biological effects (Supplementary Fig. S14).

The loss of p22 in a PTEN-functional line under hypoxic conditions resulted in decreased cell numbers (Fig. 3D), ROS levels (Supplementary Fig. S16A), as well as PTEN oxidation and Akt phosphorylation (T308) (Fig. 3E and Supplementary Fig. S17A–C). Consistently, the change in cell numbers in response to hypoxia was not observed in a PTEN-nonfunctional line (Fig. 3D). It is important to note that p22 knockdown was not able to completely protect cells from ROS production, as hypoxia most likely induces ROS production through alternative mechanisms (Bekhet and Eid, 2021). Our data suggest that NOX is a major contributor to ROS production in GBM cells, and likely to the ROS-induced effects; however, it is not the sole source of ROS. NOX-induced ROS seems to contribute to PTEN inactivation *via* oxidation and subsequent Akt phosphorylation, especially under hypoxia, resulting in elevated cell numbers under room air and low-oxygen conditions.

Radiation, a mainstay of glioma treatment, induces high levels of intracellular ROS that can ultimately result in cell death and senescence (Chen et al., 2021). However, a subpopulation of glioma cells are refractory to radiation treatment and, in fact, demonstrate enhanced stem cell-like characteristics following radiation. These cells are the likely seeds of recurrence following radiation (Ludwig and Kornblum, 2017). The NOX complex of proteins has been shown to play a role in radioresistance in a variety of tumor cells (Mortezaee et al., 2019). However, the mechanism of how NOX promotes resistance to radiation is poorly understood. We hypothesized that our proposed NOX-PTEN axis may play a role in radiation resistance. We found that a single dose of radiation significantly increased the mRNA expression of NOX4 (Fig. 4A).

Knocking down p22 resulted in decreased cell numbers following radiation only in the PTEN-functional lines (Fig. 4B), even though ROS levels were altered in both a PTEN-functional and nonfunctional line (Fig. 4C), suggesting that NOX is playing a radioprotective role in PTEN-functional GBM cells. In a PTEN-functional setting, PTEN oxidation was induced by radiation, which corresponded with an increase in Akt activation (Fig. 4D and Supplementary Fig. S18A–C). However, the radiation-induced oxidation of PTEN, and Akt activation, did not occur in the absence of p22, suggesting that the PTEN oxidation following radiation exposure of GBM cells is mediated by the NOX complex and is not a direct effect of radiation.

Consistent with our previous data, no change was seen in the PTEN-nonfunctional cells. Knocking down p22 in a PTEN-functional line enhanced the negative effects of radiation on cell numbers, whereas it made no difference in a PTEN-nonfunctional line, despite similar effects on ROS

FIG. 2. Low oxygen promotes PTEN oxidation and ROS-induced proliferation. (A) Western blot of shCON and shPTEN cells (HK157) grown under RA or 1% O_2 for 5 days indicating PTEN oxidation and total and phospho-Akt with actin used as a loading control. PTEN quantitation is of oxidized PTEN. Image is representative $n=3$. **(B)** Changes in cell number were determined with a CCK-8 assay following shCON or shPTEN treatment in three PTEN-functional lines (HK157, HK339, and HK374) and three PTEN-nonfunctional lines (HK217, HK229, and HK296) grown under RA or 1% O_2 for 5 days. Average values of all three lines were used to calculate data. $n=3$, *dots* represent individual cell lines. $^{***}p<0.01$. **(C)** Changes in ROS levels were determined with CellROX Green following shCON or shPTEN treatment in three PTEN-functional lines (HK157, HK339, and HK374) and three PTEN-nonfunctional lines (HK217, HK229, and HK296) grown under RA or 1% O_2 for 5 days. Average values of all three lines were used to calculate data. $n=3$, *dots* represent individual cell lines. $^{*}p<0.05$, $^{**}p<0.1$. **(D)** Changes in cell number were determined with a CCK-8 assay in three PTEN-functional lines (HK157, HK339, and HK374) grown under RA or 1% O_2 for 5 days and treated with NAC (1 m*M*), APO (100 μM), LY (20 μM), or H_2O_2 (10 μM). Average values of all three lines were used to calculate data. $n=3$, *dots* represent individual cell lines. $^{***}p<0.01$, $^{****}p<0.001$. **(E)** Changes in cell number were determined with a CCK-8 assay in three PTEN-nonfunctional lines (HK217, HK229, and HK296) grown under RA or 1% O_2 for 5 days and treated with NAC (1 m*M*), APO (100 μM), LY (20 μM), or H_2O_2 (10 μM). Average values of all three lines were used to calculate data. $n=3$, *dots* represent individual cell lines. $^{*}p<0.05$, $^{**}p<0.1$, $^{****}p<0.001$. **(F)** Western blot of a PTEN-functional line (HK157) grown under RA or 1% O_2 for 5 days and treated with NAC (1 m*M*), APO (100 μM), or LY (20 μM). PTEN oxidation and total and phospho-Akt with actin used as a loading control. PTEN quantitation is of oxidized PTEN. Image is representative $n=3$. APO, apocynin; RA, room air. Color images are available online.

levels (Fig. 5A, B). Since PTEN-nonfunctional cells already have increased Akt activation, NOX inhibition did not affect radiation sensitivity (Fig. 5C–D).

The above findings indicate that NOX inhibition sensitizes PTEN-functional GBM cells to radiation *in vitro*. We next tested the relevance of these findings *in vivo*. As expected, radiation treatment resulted in diminished tumor burden in mice that had been intracranially transplanted with PTEN-functional GBM cells (shCON) (Fig. 6A, B). In agreement with the *in vitro* observation, we found that knockdown of p22 alone was sufficient to diminish tumor burden. However, combining p22 knockdown with radiation resulted in a significantly reduced tumor burden in mice, relative to radiation alone (Fig. 6A, inset). This finding supports the idea that p22, and hence the NOX complex, promotes radiation resistance in GBM *in vivo*.

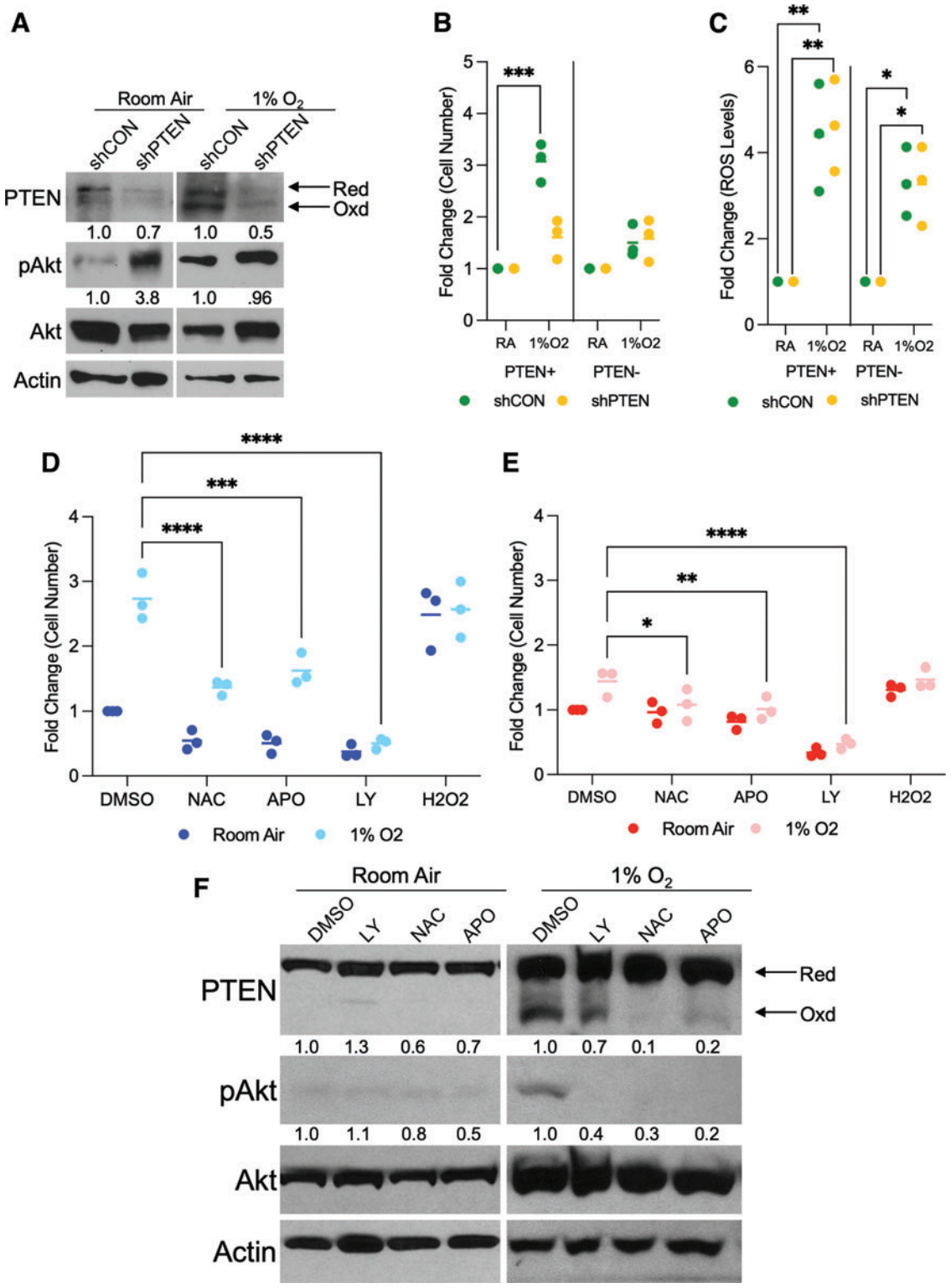

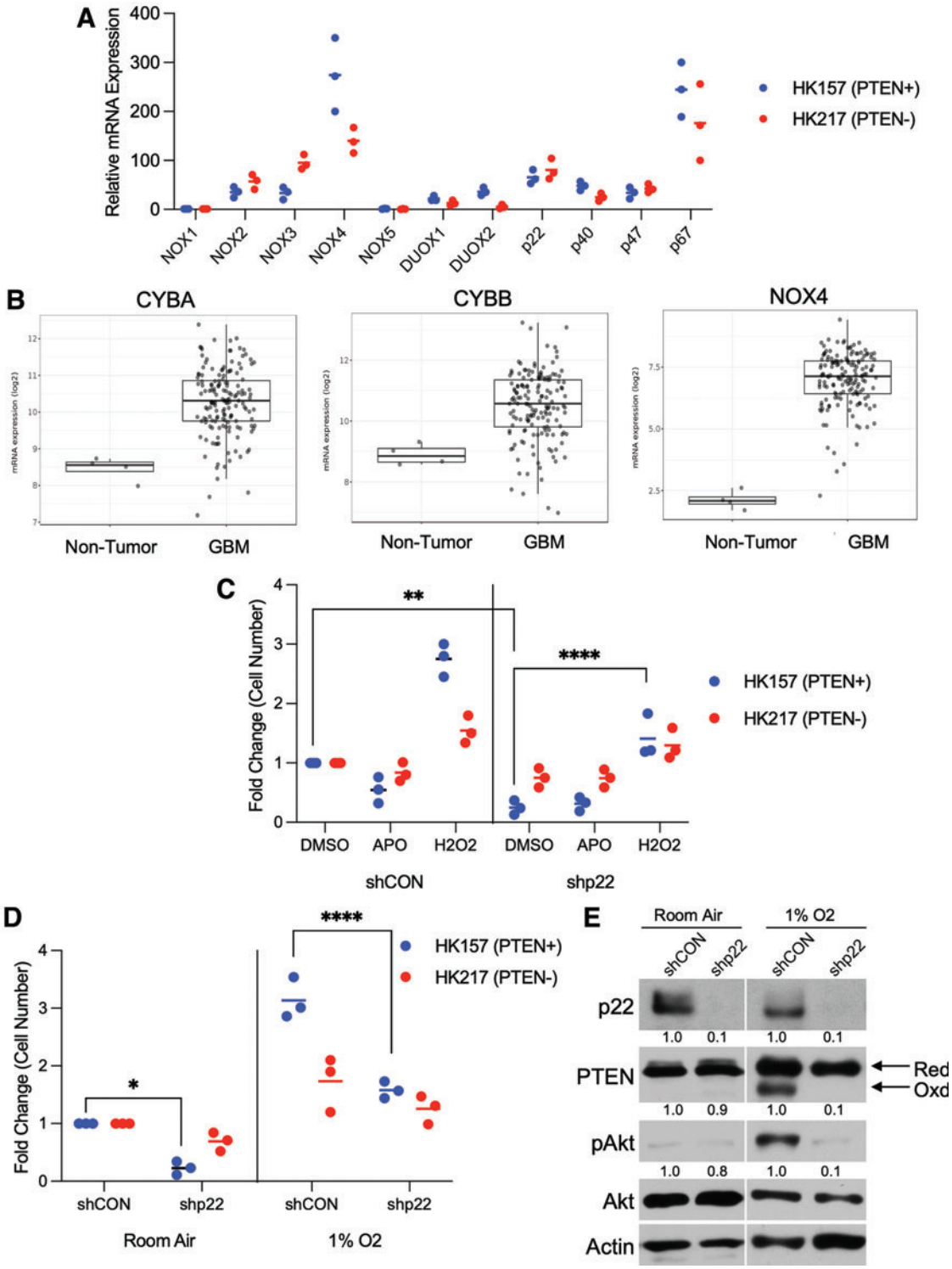

FIG. 3. NOX is expressed in GBM and regulates cell number and PTEN oxidation in low oxygen. **(A)** mRNA levels of NOX components were assessed by qRT-PCR in a PTEN-functional (HK157) and PTEN-nonfunctional (HK217) line under normal growth conditions. $n=3$, *dots* represent biological replicates. **(B)** mRNA expression of NOX2 (CYBB, P04839), NOX4 (Q9NPH5), and p22phox (CYBA, P13498) in tumor and GBM samples collected by TCGA. Data generated using GlioVis. **(C)** Changes in cell number were determined with a CCK-8 assay in a shCON or shp22 PTEN-functional (HK157) or PTEN-nonfunctional (HK217) line treated with APO (100 μM) or H_2O_2 (10 μM) for 5 days. $n=3$, *dots* represent biological replicates. $^{**}p<0.1$, $^{****}p<0.001$. **(D)** Changes in cell number were determined with a CCK-8 assay in a shCON or shp22 PTEN-functional (HK157) or PTEN-nonfunctional (HK217) line grown under room air or 1% O_2 for 5 days. $n=3$, *dots* represent biological replicates. $^{*}p<0.05$, $^{****}p<0.001$. **(E)** Western blot of a PTEN-functional line (HK157) grown under room air or 1% O_2 for 5 days following KD of p22phox. PTEN oxidation and total and phospho-Akt with actin used as a loading control. PTEN quantitation is of oxidized PTEN. Image is representative $n=4$. GBM, glioblastoma; KD, knock down; qRT-PCR, quantitative reverse transcriptase polymerase chain reaction. Color images are available online.

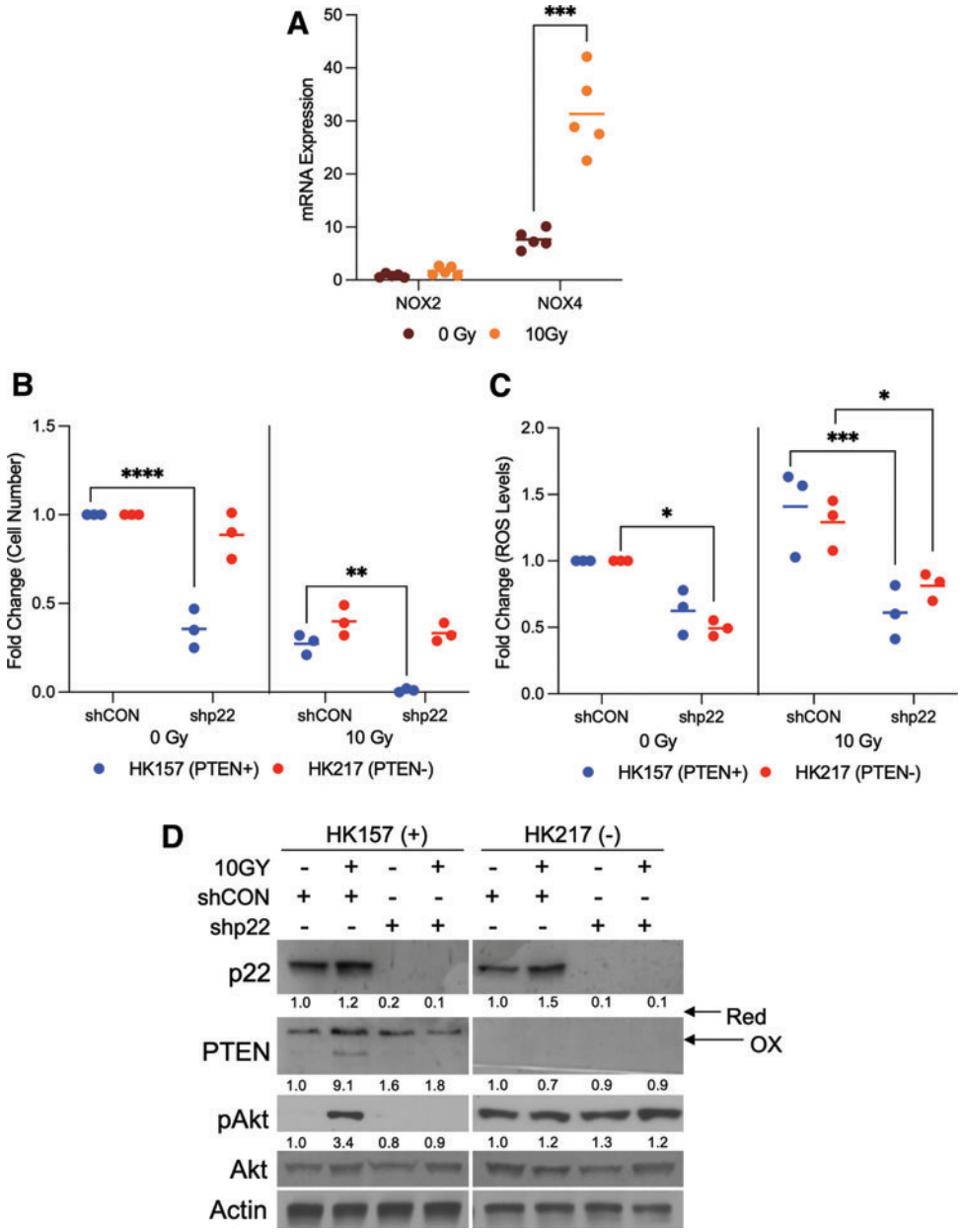

FIG. 4. Radiation activates NOX to produce ROS. **(A)** mRNA levels of NOX2 and NOX4 were assessed by qRT-PCR in a PTEN-functional cell (HK157) 24 h after exposure to 10 Gy. $n=5$, *dots* represent biological replicates. $^{***}p<0.01$. **(B)** Changes in cell number were determined with a CCK-8 assay in shCON or shp22 cells (HK157 and HK217) 5 days after exposure to 0 or 10 Gy. $n=3$, *dots* represent biological replicates. $^{**}p<0.1$, $^{****}p<0.001$. **(C)** Changes in ROS levels were determined with CellROX Green in shCON or shPTEN cells (HK157 and HK217) 5 days after exposure to 0 or 10 Gy. $n=3$, *dots* represent biological replicates. $^{*}p<0.05$, $^{***}p<0.01$. **(D)** Western blot of shCON or shp22 PTEN-functional (HK157) or PTEN-nonfunctional (HK217) cells 5 days after radiation with 0 or 10 Gy. p22phox, PTEN oxidation and total and phospho-Akt with actin used as a loading control. PTEN quantitation is of oxidized PTEN. Image is representative of $n=3$. Color images are available online.

We sacrificed all animals 4 weeks after implantation and examined the tumors for p22 expression and Akt phosphorylation and found that Akt phosphorylation was increased following radiation (Fig. 6C and Supplementary Fig. S19A, B), and this increase was lost in tumors lacking p22. Together, these data suggest that NOX activation following radiation contributes to the overall ROS levels and that in a PTEN-functional setting the NOX-generated ROS directly oxidizes and inactivates PTEN. This in turn results in elevated Akt phosphorylation, which then promotes cell proliferation and/or survival, thus contributing to the relative radiation resistance in PTEN-functional GBM tumors (Graphical Summary Illustration).

Discussion

Here we report that low oxygen or radiation oxidizes PTEN resulting in its inactivation and subsequent activation of Akt. We also show that the NOX complex is activated following radiation, and both hypoxia and radiation increase intracellular ROS levels through NOX. Finally, we found that the inhibition of the NOX pathway sensitized GBM cells to radiation both *in vitro* and *in vivo*.

Reactive oxygen species are highly reactive chemicals formed from O_2 and include peroxides, superoxides, hydroxyl radicals, and singlet oxygen. Exogenous sources of ROS include pollutants and radiation, while endogenous sources primarily come from cellular metabolism. Low levels of ROS are required for normal cellular function, while high levels of ROS promote apoptosis, autophagy, necrosis, and ferroptosis. Recently, moderate increase in ROS levels has been shown to promote tumorigenesis, invasion, and metastasis, without going high enough to induce the negative effects of ROS (Gong et al., 2022).

Given the complexity of this homeostasis, we decided to examine how moderate increases in ROS from the

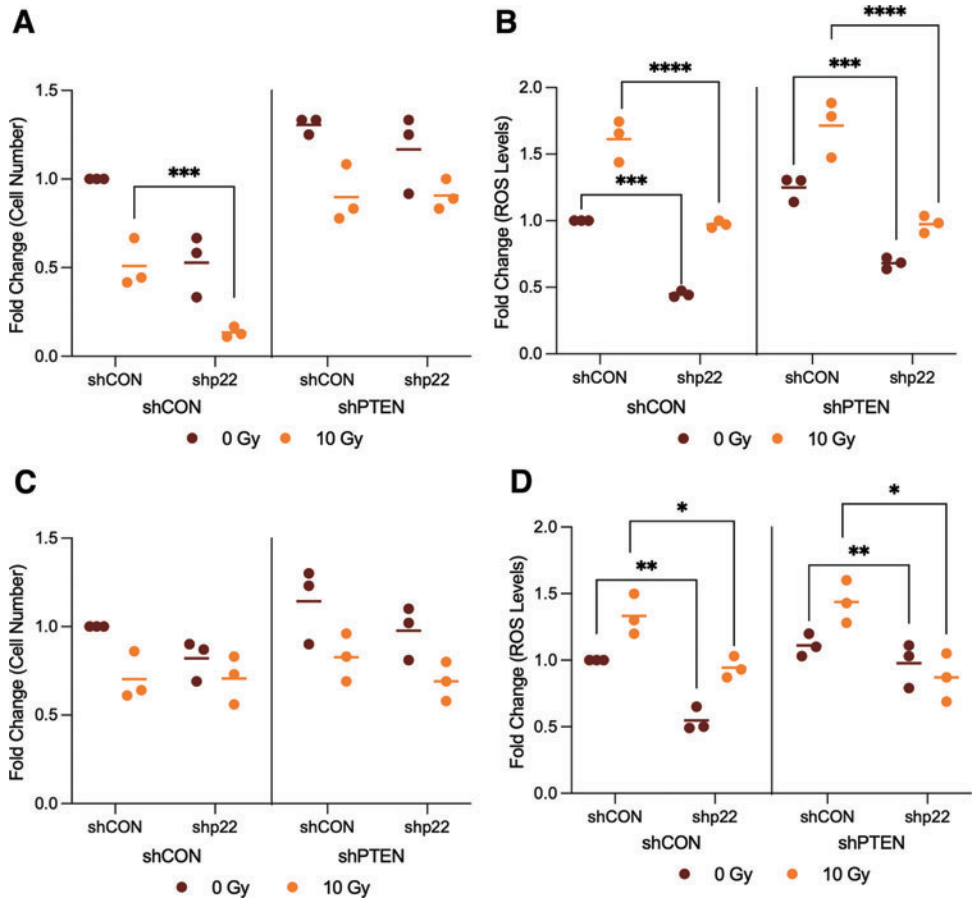

FIG. 5. Radiation activates NOX which regulates PTEN in expressing cells. (A) Changes in cell number were determined with a CCK-8 assay in shCON or shPTEN PTEN-functional (HK157) cells 5 days after exposure to 0 or 10 Gy with or without p22phox KD. $n=3$, *dots* represent biological replicates. $***p<0.01$. **(B)** Changes in ROS levels were determined with CellROX Green in shCON or shPTEN PTEN-functional (HK157) cells 5 days after exposure to 0 or 10 Gy with or without p22phox KD. $n=3$, *dots* represent biological replicates. $***p<0.01$, $****p<0.001$. **(C)** Changes in cell number were determined with a CCK-8 assay in shCON or shPTEN PTEN-nonfunctional (HK217) cells 5 days after exposure to 0 or 10 Gy with or without p22phox KD. $n=3$, *dots* represent biological replicates. **(D)** Changes in ROS levels were determined with CellROX Green in shCON or shPTEN PTEN-nonfunctional (HK217) cells 5 days after exposure to 0 or 10 Gy with or without p22phox KD. $n=3$, *dots* represent biological replicates. $*p<0.05$; $**p<0.1$. Color images are available online.

microenvironment and treatment would affect GBM growth and response to therapy. Initial experiments used NAC as an antioxidant given its ability to act as a reduced glutathione precursor and can work on a variety of free radicals (Aldini et al., 2018). Moreover, NAC has been shown in previous studies to decrease clonal neurosphere formation in adult subventricular zone cells stimulated with brain-derived neurotrophic factor (Le Belle et al., 2011). However, given the lack of precise targeting with NAC, we used the NOX inhibitor, APO, to test our hypothesis more directly.

The PTEN protein is made of two primary domains, a tyrosine phosphatase domain (which contains the active site) and a C2 domain, which binds it to the plasma membrane. In the presence of H_2O_2, a disulfide bond is formed between C71 and C124, shutting down the active site so the protein can no longer dephosphorylate PIP3, which results in prolonged activation of Akt (Zhang et al., 2020). We did not identify the specific amino acids involved in this process; however, we know that the C124 amino acid is often mutated in PTEN hamartoma tumor syndrome (PHTS), a spectrum of disorders characterized by mutations in PTEN.

The mutation at C124 mimics our system in that the protein loses its phosphatase ability. PHTS patients often have hyperactivated Akt signaling and are predisposed to tumor formation (Dragoo et al., 2021). We found that PTEN was oxidized when cells were grown under biologically relevant conditions, such as the low oxygen environment of tumors and following a single treatment with radiation. This in turn correlated with an increase in Akt activation, cell numbers, and radioresistance. Treatment with an Akt inhibitor under hypoxic conditions still resulted in PTEN oxidation; however, Akt activation and increased cell numbers were lost, suggesting that the PTEN/Akt pathway is required for the biological effects reported in this article.

While some GBM express virtually no functional PTEN, due to loss of heterozygosity (70%), mutation (40%), or both, many express functional PTEN protein or only have PTEN mutations in one allele. However, the vast majority of tumors exhibit at least some activation of the PI3K pathway (Verhaak et al., 2010). While a number of different mechanisms can promote downstream Akt and mTOR activity, including cross talk from the mitogen-activated pathway (MAPK),

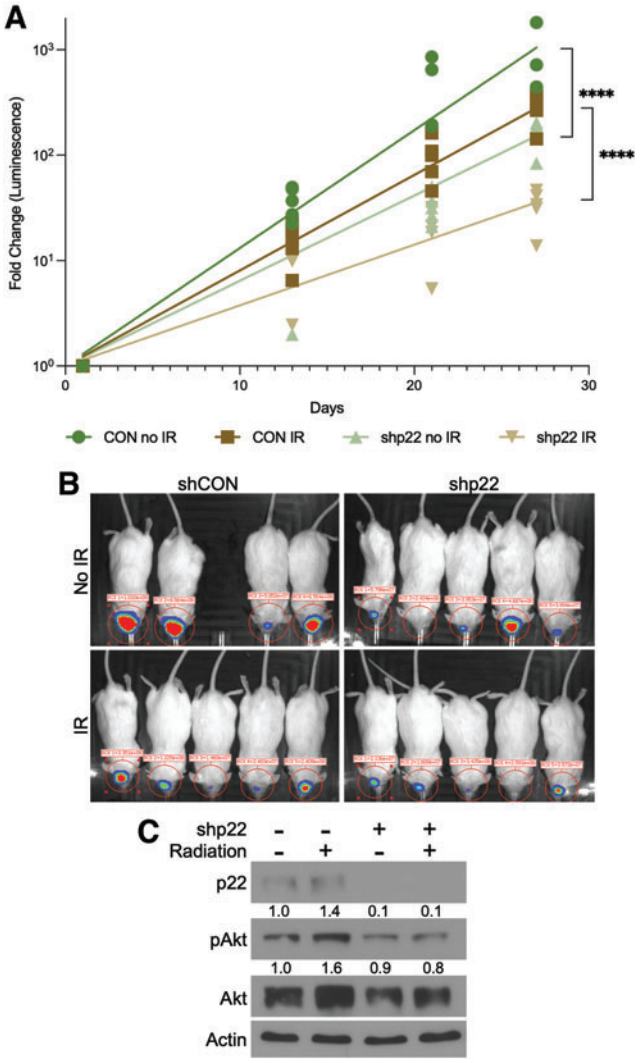

FIG. 6. NOX promotes radioresistance *in vivo*. **(A)** Tumor volume was assessed using luminescence from shCON or shp22 GFP-FLUC xenograft intracranial tumors (HK408) at different time points following a single dose of radiation. *Dots* represent individual mice. ****$p < 0.001$. **(B)** Images of different treatment groups on day 21 following radiation. **(C)** Western blot of shCON or shp22 nonperfused xenograft intracranial tumors (HK408) 28 days after radiation. Image is representative of $n = 3$. FLUC, firefly luciferase; GFP, green fluorescent protein. Color images are available online.

direct mutations in PI3 kinases, and other relevant proteins (Ludwig and Kornblum, 2017), our data suggest that the hypoxic environment of the tumor may play a role in activation of this pathway, and thus, antioxidant treatment may be an interesting direction of research—one that might seem counterintuitive at first glance.

In fact, others have found that curcumin (an antioxidant) is able to sensitize GBM cells to radiation through a variety of pathways (Zoi et al., 2022). However, our study would suggest that at least some residual PTEN activity would be required for a significant therapeutic effect. We do not yet know whether functional PTEN is required for the protumorigenic role of ROS in other cancers.

One of the primary sources of endogenous ROS is the NOX complex of proteins found at and within cell membranes. Increased activation or expression of one or several NOX member proteins has been reported in multiple cancers corresponding with increased tumorigenicity and resistance to treatment (Mortezaee et al., 2019). Previous studies have demonstrated that the activation of NOX results in enhanced NSC self-renewal and enhanced neurogenesis in a PTEN-dependent manner (Le Belle et al., 2011). Although it is unclear whether brain tumors are derived from NSC, we reasoned that the shared properties of neural stem and GBM stem cells might extend to a shared mechanism of ROS-induced survival.

While our cultures are enriched in GSC, consistent with this link, it must be noted that we did not demonstrate a GSC-specific effect in the current study. The current study goes beyond the notion that PTEN is required for the effects of NOX activation in glioma and NSC, but that under physiological conditions in which NOX is activated, such as during hypoxia, PTEN is oxidized and inactivated, leading to the activation of Akt. Further studies will be required to determine whether there are distinct functional differences between the effects of NOX activation and outright PTEN deletion in GBM.

The induction of ROS is the main underlying mechanism of radiotherapy, and several prior studies have found that inhibition of NOX increases sensitivity to radiation. However, the mechanism of action of this affect has yet to be elucidated (Teixeira et al., 2017). In this study, we demonstrated that radiation induces NOX mRNA and activates NOX, which, in turn, oxidizes PTEN, ultimately leading to downstream activation of Akt and enhanced cell production *in vitro* and enhanced tumor growth *in vivo*. These findings support the concept of NOX inhibition as an adjunct to radiation therapy in PTEN-replete tumors.

In fact, because of the importance of the NOX family of proteins, in several disorders, including cancer and stroke, a great deal of effort has gone into developing pharmacological NOX inhibitors. Recently, the World Health Organization approved a new terminology stem, ''naxib,'' which refers to NADPH oxidase inhibitor and thereby recognized NOX inhibitors as a new therapeutic class (Elbatreek et al., 2021). With the development of these and other drugs, it may eventually be possible to supplement radiation treatment for PTEN-positive GBM patients with an NOX inhibitor and see improved outcomes.

There are several limitations to our study. First, we do not yet know whether the NOX system is truly expressed in GBM cells in human tumors *in situ*. While NOX2 and NOX4 are expressed in GBM, review of single cell studies reveals limited expression of the mRNA for NOX components within tumor cells (Darmanis et al., 2017). However, we do not know whether this limited expression is sufficient to play a direct role in tumor biology in humans or whether NOX is induced by radiation in human GBM cells undergoing therapeutic radiation. It is possible that NOX is upregulated by the act of growing them in GSC-enriched gliomasphere cultures and that this upregulation is maintained during *in vivo* growth in xenografts.

It is possible that human brain tumors, including those undergoing radiation, receive ROS *via* non-cell autonomous activation of other cells in the microenvironment, including myeloid and vascular cells (Bekhet and Eid, 2021), both of which express abundant mRNA for NOX components (Darmanis et al., 2017). We also recognize that there are

many different sources and types of free radicals, and this article looks at only a small subset of possibilities.

Another limitation of our current study is in the dose and schedule of radiation used. We chose a single, high dose of radiation, rather than a fractionated schedule as is administered to people (Ziu et al., 2020). Murine xenografts and human tumors *in situ* are of vastly different sizes (Ma et al., 2020; Rutter et al., 2017). A radiation dose that kills a large percentage of cells may leave tens of millions of cells leftover in a human tumor, and only a few cells left in a murine tumor, thus making it unlikely to be able to observe tumor growth and regrowth following radiation over the life span of a mouse. Future preclinical studies using either large animal models or alternate dosing schedules may be required before therapeutic human trials with NOX inhibitors and GBM radiation.

A final limitation to the current study is that we focus only on NOX-generated ROS and did not investigate the potential effects of other forms of ROS. Furthermore, our studies do not investigate the detailed mechanisms by which NOX may be activated. For example, NOX is activated by RAC1, which is known to function in several different pathways related to cell survival (Mosaddeghzadeh and Ahmadian, 2021). Downstream studies would be needed to investigate whether RAC1 is a key regulator of NOX in GBM. Despite these limitations, our study provides a strong basis for pursuing NOX inhibition in PTEN-expressing GBM cells as a possible adjunct to radiation therapy.

Materials and Methods

Tissue culture

The isolation and propagation of the primary GSC containing cultures (gliomaspheres) used for this study were described previously (Laks et al., 2016). The prior study also describes the patient characteristics for each line used. Briefly, to culture the cells, on the day of resection, samples were digested with TrypLE and further dissociated mechanically. Acellular debris was removed, and the remaining cells were incubated in gliomasphere media (Dulbecco's modified Eagle's medium/F12 supplemented with B27, penicillin–streptomycin, heparin, EGF, and basic FGF) for several days until spheres began to form. Frozen stocks were made at passage 5 to maintain cells at low passage. Cell cultures were maintained as previously described (Laks et al., 2009). For hypoxia experiments, cells were acclimated to low oxygen for 2 weeks before experiments.

Drug treatment

Cells were plated according to their assay at a density of 100,000 cells/mL and allowed to settle for 24 h. After that time, cells were treated with a single dose of the following drugs: H_2O_2, NAC, LY-294002 (LY), or APO, and most experiments were run after 5 days.

Immunofluorescence staining and quantitation

For immunostaining, cells were first fixed in 4% paraformaldehyde for 15 min. Following fixation, cells were washed with phosphate-buffered saline (PBS), permeabilized with PBS with 0.1% Triton X-100 for nuclear staining, and blocked in PBS with 2% bovine serum albumin at room temperature for 30 min. Cells were then incubated with the indicated primary antibodies: NOX2 (1:100, PA5-79118; Thermo Fisher Scientific, Waltham, MA), NOX4 (1:100, MAB8158; R&D Systems, Minneapolis, MN), and CYBA/P22 (1:100, PA5-71642; Thermo Fisher Scientific) overnight at 4°C. Cells were washed with PBS and incubated with species-appropriate goat/donkey secondary antibodies coupled to Alexa Fluor dye 568 (Invitrogen, Waltham, MA) and Hoechst dye for nuclear staining for 2 h at room temperature. Stained cells were imaged using EVOS Cell Imaging systems microscope (Thermo Fisher Scientific), and quantification was performed using ImageJ.

Growth assay

Cells were grown at a density of 100,000 cell/mL and allowed to grow for the appropriate time following treatment. On the day of experiment, spheres were treated with Cell Counting Kit-8 (CCK-8; Dojindo, Rockville, MD) according to the manufacturer's protocol. Results were read with a microplate reader on a Varioskan Lux multimode plate reader, and absorbance was recorded at 450 nm. In early experiments, cells were counted with trypan blue exclusion and read on a cell countess. To facilitate data acquisition, we performed subsequent studies with the CCK-8 system. Initially, we tested the validity of the system by comparing it with trypan blue when cells were treated with H_2O_2, radiation, and hypoxia (Supplementary Fig. S20A–F).

Western blots

Proteins from the cell lines were extracted in RIPA buffer and quantitated by Bio-Rad protein assay. Equal amounts of total proteins were loaded on sodium dodecyl sulfate–polyacrylamide gel electrophoresis (SDS-PAGE) gels, transferred onto a nitrocellulose membrane, and probed with primary antibodies (anti-PTEN [138G6; Cell Signaling, Danvers, MA], anti-actin [EPR16769; Abcam, Cambridge, United Kingdom], anti-p22phox [ab191512; Abcam], anti-Akt [C67E7; Cell Signaling], and anti-phospho-Akt T308 [D255E6; Cell Signaling]) overnight at 4°C. Horseradish peroxidase-conjugated secondary antibodies were incubated for 1 h at room temperature. Proteins were visualized by chemiluminescence as recommended by the manufacturer (Thermo Fisher Scientific). PTEN oxidation was assessed according to Delgado-Esteban et al. (2007). Films were superimposed on the membrane to visualize molecular markers and identify bands. Original versions of all Western blot are provided in Supplementary Figures S21–S27.

Animal strains, intracranial xenotransplantation, and optical imaging

All animal studies were performed according to approved protocols by the Institutional Animal Care and Use Committee at the UCLA. Studies did not discriminate sex, and both male and females were used. Eight- to 12-week-old NOD-SCID gamma null mice were used to generate tumors from a patient-derived GBM line HK408 5×10^4 tumor cells containing a firefly luciferase–green fluorescent protein (FLUC-GFP) lentiviral construct were injected intracranially into the neostriatum in mice. Tumor growth was monitored at 2, 3, and 4 weeks after transplantation using IVIS Lumina II bioluminescence imaging at the Crump Institute for Molecular Imaging at UCLA.

Mice were anesthetized by inhalation of isoflurane. Intraperitoneal injection of 100 μL of luciferin (30 mg/mL) was followed by 10 min of live uptake to interact with the

luciferase-expressing FLUC-GFP tumor cells and produce bioluminescence. The IVIS Lumina 2 imaging system (Caliper Life Sciences, Hopkinton, MA) was utilized to photograph the mice, and images were overlaid with a color scale of a region of interest representing total flux (photon/second) and quantified with the Living Image software package (Xenogen, Alameda, CA).

ROS measurement

Cells were grown at a density of 100,000 cell/mL and allowed to grow for the appropriate time following treatment. On the day of experiment, spheres were dissociated with Accumax (Innovative Cell Technologies), and live cells were counted using a Countess Automated Cell Counter (Life Technologies, Carlsbad, CA), with 0.4% trypan blue exclusion. Fifty thousand cells were treated with CellROX Green (Thermo Fisher, Waltham, MA) according to the manufacturer's protocol. Cells were then counterstained with Hoechst 33342 (Thermo Fisher) to use as a loading control for calculations. Cells were loaded into a 96-well black well plate and read on a Varioskan Lux multimode plate reader, and fluorescence was recorded at the appropriate wavelengths.

Irradiation of glioma cultures and orthotopic tumor xenografts

Cultured cells were irradiated at room temperature using an experimental X-ray irradiator (Gulmay Medical, Inc., Atlanta, GA) at a dose rate of 5.519 Gy/min for the time required to apply a prescribed dose. The X-ray beam was operated at 300 kV and hardened using a 4-mm Be, a 3-mm Al, and a 1.5-mm Cu filter and calibrated using NIST-traceable dosimetry. Tumor-bearing mice were irradiated at a single dose of 10 Gy using an image-guided small animal irradiator (X-RAD SmART; Precision X-Ray, North Branford, CT) with an integrated cone beam CT (60 kVp, 1 mA) and a bioluminescence imaging unit as described previously (Bhat et al., 2020). Individual treatment plans were calculated for each animal using the SmART-Plan treatment planning software (Precision X-Ray). Radiation treatment was applied using a 5×5 mm collimator from a lateral field.

qRT-PCR

RNA was isolated using TRIzol (Gibco, Waltham, MA), and 1.5 μg RNA was converted to cDNA by reverse transcription. qRT-PCR was performed after the addition of Power SYBR Master Mix (Applied Biosystems, Foster City, CA) on an ABI PRISM 7700 sequence detection system (Applied Biosystems).

shRNA

Lentiviral-mediated shRNA knockdowns of *PTEN* and *p22-phox* were performed using constructs from the Dharmacon-Harmon (Lafayette, CO) library. Four shPTEN constructs and five shp22-phox constructs were tested, and one of each was chosen following examination of knockdown efficiency and resulting phenotype. Briefly, virus was made using HEK-293T cells transfected with package, envelope, and the shRNA construct using Lipofectamine (Thermo Fisher) in the absence of serum or antibiotics. Conditioned media from the cells were collected 3 days later and added to the GBM cell line of interest.

Statistics

GraphPad Prism 9 was used for statistical analyses. p values (adjusted in the case of multiple comparisons) <0.05 were considered significant. Comparisons between groups were initially evaluated by one-, two-, or three-way analysis of variance with *post hoc* Šídák's multiple comparisons tests. Multiple unpaired t-tests with the Holm–Šídák correction were used to compare gene expression data in Figures 3A and 4A. For *in vivo* tumor growth data in figure, data were fit by nonlinear regression, and slopes were compared across groups: $*p < 0.05$, $**p < 0.1$, $***p < 0.01$, $****p < 0.001$.

Data collection

Electronic laboratory notebook was not used.

Authors' Contributions

K.L., S.D.M., M.C., and J.S. designed, performed, and analyzed the experiments. J.E.L.B., E.V., F.P., and H.L.K. conceived and conceptualized the study. K.L., S.D.M., M.C., and H.I.K. wrote the article. All authors reviewed the article.

Author Disclosure Statement

No competing financial interests exist.

Funding Information

This work was supported by the Dr. Miriam and Sheldon G. Adelson Medical Research Foundation.

Supplementary Material

Supplementary Figure S1
Supplementary Figure S2
Supplementary Figure S3
Supplementary Figure S4
Supplementary Figure S5
Supplementary Figure S6
Supplementary Figure S7
Supplementary Figure S8
Supplementary Figure S9
Supplementary Figure S10
Supplementary Figure S11
Supplementary Figure S12
Supplementary Figure S13
Supplementary Figure S14
Supplementary Figure S15
Supplementary Figure S16
Supplementary Figure S17
Supplementary Figure S18
Supplementary Figure S19
Supplementary Figure S20
Supplementary Figure S21
Supplementary Figure S22
Supplementary Figure S23
Supplementary Figure S24
Supplementary Figure S25
Supplementary Figure S26
Supplementary Figure S27

References

Aldini G, Altomare A, Baron G, et al. N-acetylcysteine as an antioxidant and disulphide breaking agent: The reasons why. Free Radic Res 2018;52(7):751–762; doi: 10.1080/10715762.2018.1468564

Bekhet OH, Eid ME. The interplay between reactive oxygen species and antioxidants in cancer progression and therapy: A narrative review. Transl Cancer Res 2021;10(9):4196–4206; doi: 10.21037/tcr-21-629

Bhat K, Saki M, Vlashi E, et al. The dopamine receptor antagonist trifluoperazine prevents phenotype conversion and improves survival in mouse models of glioblastoma. Proc Natl Acad Sci U S A 2020;117(20):11085–11096; doi: 10.1073/pnas.1920154117

Bowman RL, Wang Q, Carro A, et al. GlioVis data portal for visualization and analysis of brain tumor expression datasets. Neurooncology 2017;19(1):139–141; doi: 10.1093/neuonc/now247

Cao W, Zhou Q, Wang H, et al. Hypoxia promotes glioma stem cell proliferation by enhancing the 14-3-3β expression via the PI3K pathway. J Immunol Res 2022;2022:5799776; doi: 10.1155/2022/5799776

Chen Y, Li Y, Huang L, et al. Antioxidative stress: Inhibiting reactive oxygen species production as a cause of radioresistance and chemoresistance. Oxid Med Cell Longev 2021;2021:6620306; doi: 10.1155/2021/6620306

Darmanis S, Sloan SA, Croote D, et al. Single-cell RNA-seq analysis of infiltrating neoplastic cells at the migrating front of human glioblastoma. Cell Rep 2017;21(5):1399–1410; doi: 10.1016/j.celrep.2017.10.030

Delgado-Esteban M, Martin-Zanca D, Andres-Martin L, et al. Inhibition of PTEN by peroxynitrite activates the phosphoinositide-3-kinase/Akt neuroprotective signaling pathway. J Neurochem 2007;102(1):194–205; doi: 10.1111/j.1471-4159.2007.04450.x

Dragoo DD, Taher A, Wong VK, et al. PTEN Hamartoma tumor syndrome/Cowden syndrome: Genomics, oncogenesis, and imaging review for associated lesions and malignancy. Cancers (Basel) 2021;13(13):3120; doi: 10.3390/cancers13133120

Elbatreek MH, Mucke H, Schmidt HHHW. NOX inhibitors: From bench to naxibs to bedside. Handb Exp Pharmacol 2021;264:145–168; doi: 10.1007/164_2020_387

Gong S, Wang S, Shao M. NADPH oxidase 4: A potential therapeutic target of malignancy. Front Cell Dev Biol 2022;10:884412; doi: 10.3389/fcell.2022.884412

Groszer M, Erickson R, Scripture-Adams DD, et al. Negative regulation of neural stem/progenitor cell proliferation by the Pten tumor suppressor gene in vivo. Science 2001;294(5549):2186–2189; doi: 10.1126/science.1065518

Groszer M, Erickson R, Scripture-Adams DD, et al. PTEN negatively regulates neural stem cell self-renewal by modulating G0-G1 cell cycle entry. Proc Natl Acad Sci U S A 2006;103(1):111–116; doi: 10.1073/pnas.0509939103

Hemmati HD, Nakano I, Lazareff JA, et al. Cancerous stem cells can arise from pediatric brain tumors. Proc Natl Acad Sci U S A 2003;100(25):15178–15183; doi: 10.1073/pnas.2036535100

Laks DR, Crisman TJ, Shih MYS, et al. Large-scale assessment of the gliomasphere model system. Neurooncology 2016;18(10):1367–1378; doi: 10.1093/neuonc/now045

Laks DR, Masterman-Smith M, Visnyei K, et al. Neurosphere formation is an independent predictor of clinical outcome in malignant glioma. Stem Cells Dayt Ohio 2009;27(4):980–987; doi: 10.1002/stem.15

Le Belle JE, Orozco NM, Paucar AA, et al. Proliferative neural stem cells have high endogenous ROS levels that regulate self-renewal and neurogenesis in a PI3K/Akt-dependant manner. Cell Stem Cell 2011;8(1):59–71; doi: 10.1016/j.stem.2010.11.028

Le Belle JE, Sperry J, Ngo A, et al. Maternal inflammation contributes to brain overgrowth and autism-associated behaviors through altered redox signaling in stem and progenitor cells. Stem Cell Rep 2014;3(5):725–734; doi: 10.1016/j.stemcr.2014.09.004

Lee S-R, Yang K-S, Kwon J, et al. Reversible inactivation of the tumor suppressor PTEN by H2O2. J Biol Chem 2002;277(23):20336–20342; doi: 10.1074/jbc.M111899200

Ludwig K, Kornblum HI. Molecular markers in glioma. J Neurooncol 2017;134(3):505–512; doi: 10.1007/s11060-017-2379-y

Ma Z, Niu B, Phan TA, et al. Stochastic growth pattern of untreated human glioblastomas predicts the survival time for patients. Sci Rep 2020;10(1):6642; doi: 10.1038/s41598-020-63394-w

Mortezaee K, Goradel NH, Amini P, et al. NADPH oxidase as a target for modulation of radiation response; implications to carcinogenesis and radiotherapy. Curr Mol Pharmacol 2019;12(1):50–60; doi: 10.2174/1874467211666181010154709

Mosaddeghzadeh N, Ahmadian MR. The RHO family GTPases: Mechanisms of regulation and signaling. Cells 2021;10(7):1831; doi: 10.3390/cells10071831

Rodriguez SMB, Staicu G-A, Sevastre A-S, et al. Glioblastoma stem cells-useful tools in the battle against cancer. Int J Mol Sci 2022;23(9):4602; doi: 10.3390/ijms23094602

Rutter EM, Stepien TL, Anderies BJ, et al. Mathematical analysis of glioma growth in a murine model. Sci Rep 2017;7(1):2508; doi: 10.1038/s41598-017-02462-0

Su X, Yang Y, Guo C, et al. NOX4-derived ROS mediates TGF-B1-induced metabolic reprogramming during epithelial-mesenchymal transition through the PI3K/AKT/HIF-1α pathway in glioblastoma. Oxid Med Cell Longev 2021;2021:5549047; doi: 10.1155/2021/5549047

Teixeira G, Szyndralewiez C, Molango S, et al. Therapeutic potential of NADPH oxidase 1/4 inhibitors. Br J Pharmacol 2017;174(12):1647–1669; doi: 10.1111/bph.13532

Verhaak RGW, Hoadley KA, Purdom E, et al. Integrated genomic analysis identifies clinically relevant subtypes of glioblastoma characterized by abnormalities in PDGFRA, IDH1, EGFR, and NF1. Cancer Cell 2010;17(1):98–110; doi: 10.1016/j.ccr.2009.12.020

Vermot A, Petit-Härtlein I, Smith SME, et al. NADPH oxidases (NOX): An overview from discovery, molecular mechanisms to physiology and pathology. Antioxid Basel Switz 2021;10(6):890; doi: 10.3390/antiox10060890

Vilar JB, Christmann M, Tomicic MT. Alterations in molecular profiles affecting glioblastoma resistance to radiochemotherapy: Where does the good go? Cancers (Basel) 2022;14(10):2416; doi: 10.3390/cancers14102416

Zhang Y, Park J, Han S-J, et al. Redox regulation of tumor suppressor PTEN in cell signaling. Redox Biol 2020;34:101553; doi: 10.1016/j.redox.2020.101553

Ziu M, Kim BYS, Jiang W, et al. The role of radiation therapy in treatment of adults with newly diagnosed glioblastoma multiforme: A systematic review and evidence-based clinical practice guideline update. J Neurooncol 2020;150(2):215–267; doi: 10.1007/s11060-020-03612-7

Zoi V, Galani V, Tsekeris P, et al. Radiosensitization and radioprotection by curcumin in glioblastoma and other cancers. Biomedicines 2022;10(2):312; doi: 10.3390/biomedicines 10020312

Address correspondence to:
Dr. Harley I. Kornblum
The Intellectual and Developmental Disabilities Research Center
Department of Psychiatry and Biobehavioral Sciences
David Geffen School of Medicine at UCLA
Room 341 NRB
635 Charles East Young Drive South
Los Angeles, CA 90095
USA

E-mail: hkornblum@mednet.ucla.edu

Date of first submission to ARS Central, August 1, 2022; date of final revised submission, June 9, 2023; date of acceptance, June 21, 2023.

Abbreviations Used

Akt = protein kinase B
APO = apocynin
CCK-8 = cell counting kit-8
EGF = epidermal growth factor
FGF = fibroblast growth factor
FLUC-GFP = firefly luciferase–green fluorescent protein
GBM = glioblastoma
GSC = glioma stem cell
H_2O_2 = hydrogen peroxide
KD = knock down
mTOR = mammalian target of rapamycin
NAC = *N*-acetylcysteine
NADPH = nicotinamide adenine dinucleotide phosphate
NOX = NADPH oxidase
NSC = neural stem cell
PBS = phosphate-buffered saline
PHTS = PTEN hamartoma tumor syndrome
PI3K = phosphoinositide 3-kinase
PTEN = phosphate and tensin homolog
qRT-PCR = quantitative reverse transcription polymerase chain reaction
RA = room air
ROS = reactive oxygen species
SDS-PAGE = sodium dodecyl sulfate–polyacrylamide gel electrophoresis